

Military Technical College

Kobry El-Kobbah,

Cairo, Egypt



**12th International Conference
on Civil and Architecture
Engineering**

ICCAE-12-2018

Behavior of post and pre-heated RC short columns wrapped with ferrocement

Israa Abd Elhady¹, Mahmoud Elsayed¹, Alaa Elsayed^{1*}

¹Department of Civil Engineering, Faculty of Engineering Fayoum University, Fayoum, Egypt

Corresponding author E-mail: alaa_elsayed2009@yahoo.com

Abstract

In this work, experimental and numerical studies were carried out to investigate the behavior of pre- and post-heated RC short columns wrapped by ferrocement overlays. Ten RC columns were constructed and tested experimentally under axial load. The tested columns were divided into unheated columns, post-heated columns, post-heated columns repaired with ferrocement, and heated wrapped columns. All heated columns were heated at a temperature of 300°C for 3 hours. The experimental results were utilized for validation of the finite element models which developed by using ANSYS 13 software package. Based on the experimental and numerical results it is suggested that an equation that could predict the ultimate load of post heated RC short columns wrapped by ferrocement. Afterwards, a wide range of the analysis was conducted models were analyzed to observe the effect of other parametric studies on the enhancement of axial load of post-heated columns confined by ferrocement. The results of the design equation were mutually compared with both the experimental and numerical ones. The research proved that the repairing scheme has an efficiency in surpassing the failure load of and improving the ultimate strength of heated columns significantly. The results of both the finite element and the prediction of the equation gave a satisfactory agreement with experimental ones.

Keywords: Strengthening, RC columns, Heat, Ferrocement, ANSYS

1. Introduction

Columns are considered one of the main structural elements within concrete structures. As they form the main support for other load bearing elements, e.g. beams and slabs. Their collapse during a fire can be detrimental to the stability of the rest of the structure. Consequently, cracking and spalling of concrete columns after a fire exposure are often accompanied with the corrosion of internal steel reinforcement. Furthermore, drastic reduction occurred in load carrying capacities of the columns after being exposed to fire. Inevitably, it is urgently needed to strengthen and rehabilitate such columns. The most common and traditional techniques of repairing columns are to bond steel plates or enlarge the column cross-section using concrete jackets. However, there are other advanced methods to strengthen and repair columns, such as FRP, which is an expensive technique that mandates complex application procedures. Ferrocement has been currently used

to strengthen concrete elements as an alternative repair material due to its ease of application as well as low cost. Ferrocement is a form of reinforced concrete that is made of a single or multiple layers of wire mesh and/or small-diameter rods completely encapsulated in mortar [1]. Numerous experimental and numerical studies were performed to evaluate the performance of strengthening schemes on the behaviour of RC columns exposed to high temperatures. Significant studies have been investigated the influence of utilising ferrocement confinement in strengthening and repairing RC columns [2-11]. In general, the results indicated that the strength and deformability of RC columns could be enhanced by encased ferrocement. Many studies [12-19] investigated experimentally the efficiency of using FRP, CFRP, and GFRP as strengthening techniques to repair RC columns exposed to different elevated temperature rates. The experimental results proved that wrapping RC columns with FRP scheme improve the ultimate load carrying capacities and enhance the ductility. Al-Kamaki et al. [20] carried out an experimental and numerical study on the behaviour of heated RC columns encased in CFRP. Also, El-Karmoty [21] carried out an experimental and theoretical study on the response of thermal protection of RC retrofitted by GFRP overlays. Tetta and Dionysios [22] studied the performance of TRM and FRP wrapping in the shear strengthening of RC beams exposed to different levels of temperature. Yaqub et al. [23] carried out an experimental study to investigate the behaviour of post-heated RC columns enveloped with FRP composites. Yaqub and Bailey [24] and Bailey and Yaqub [25] studied experimentally the behaviour of post-heated RC square and circular columns wrapped with glass or carbon fibre reinforced polymers. Yaqub et al. [26] carried out an experimental investigation to evaluate the efficiency of using ferrocement and fibre reinforced FRP jackets for the repair of the post-heated square and circular reinforced concrete columns.

2. Research significance

The aim of this work is to investigate the efficiency of using ferrocement confinement in repairing heated RC columns. In order to do that, ten RC columns were tested experimentally. The phases of laboratory program included columns which were unheated, post-heated, repaired post-heated with ferrocement jacket and wrapped columns with ferrocement subsequent heated (pre-heated). Then, numerical analysis and predicted formula were performed to determine the ultimate load carrying capacities of tested columns. Finally, nonlinear finite element models were developed to cover other parameters which were not studied experimentally.

3. Experimental Program

4.1 Material Properties

The same batch of the concrete mix was used for all columns to preserve the same strength of concrete. The concrete mixing compositions were 350 kg/m³ cement, 170 kg/m³ free water, 650 kg/m³ fine aggregate, and 1170 kg/m³ coarse aggregate. The average compressive strength of concrete was 27 MPa at 28 days. The proportion of the ferrocement mortar mixes was 1:0.4:2 of the cement, water, and sand, respectively. A total of 1.5% super plasticizer and 15% of silica-fume by weight of cement were added to improve the workability and the strength of the matrix. The average mortar grade at the time of testing was 37 MPa. The mix ratio for concrete was 1:0.48:1.28:2.17 of cement, water, fine and coarse aggregate, respectively. The average compressive strength of concrete was 27 MPa at 28 days. The ratio of the mortar mixture was 1:0.4:2 of the cement, water, and sand, respectively. A total of 1.5% super plasticizer and 15% of silica-fume by weight of cement were added to improve the workability and the strength of the matrix. The average mortar strength was 35 MPa at 28 days.

Three different types of reinforcing steel bars were used as shown in Table 1. Expanded wire mesh (diamond) was used as a ferrocement reinforcement jacket. The diameter of wires in the mesh was 1.35 mm and diameter 28 mm X 16 mm wire spacing. The yield strength and modulus of elasticity of individual wires of the mesh were 370 MPa and 175000 MPa respectively.

Table 1: Properties of steel reinforcement.

Bar name	Actual Diameter (mm)	Actual area (mm ²)	Yield Strength (MPa)	Ultimate Strength (MPa)	Young's Modulus (MPa)
Ø 6mm	6	28.3	282	459	195000
Φ 10 mm	9.91	77.1	412	628	195000
Φ 16 mm	15.85	197.2	412	628	195000

Test Specimens

In order to evaluate the efficiency of applying ferrocement overlays in repaired RC columns exposed to fire, ten RC columns were constructed and tested experimentally. The schematic experimental layout consists of the cast and cure the RC columns, heated them to temperature, wrap them with ferrocement and then test the specimens under axial load. All the specimens have the same square cross-section of 150 mm and a height equivalent to a 1000 mm. The specimens were equally divided into two groups, of five columns each, based on the longitudinal reinforcement. The first group have 4Φ10 mm and second one have 8Φ16 mm which corresponds to a longitudinal reinforcement ratio was 1.3% and 7%, respectively. All columns have the same number and arrangement of stirrups. The columns geometry, reinforcement, and properties of the control, as well as the confined columns, are plotted in Fig. 1. The specimens were tested under four different conditions described in the sequel:

- (a) Two unheated columns without ferrocement jacket;
- (b) Two heated columns without repairing;
- (c) Two wrapped columns with heating;
- (d) Four heated and repaired columns with ferrocement jacket.

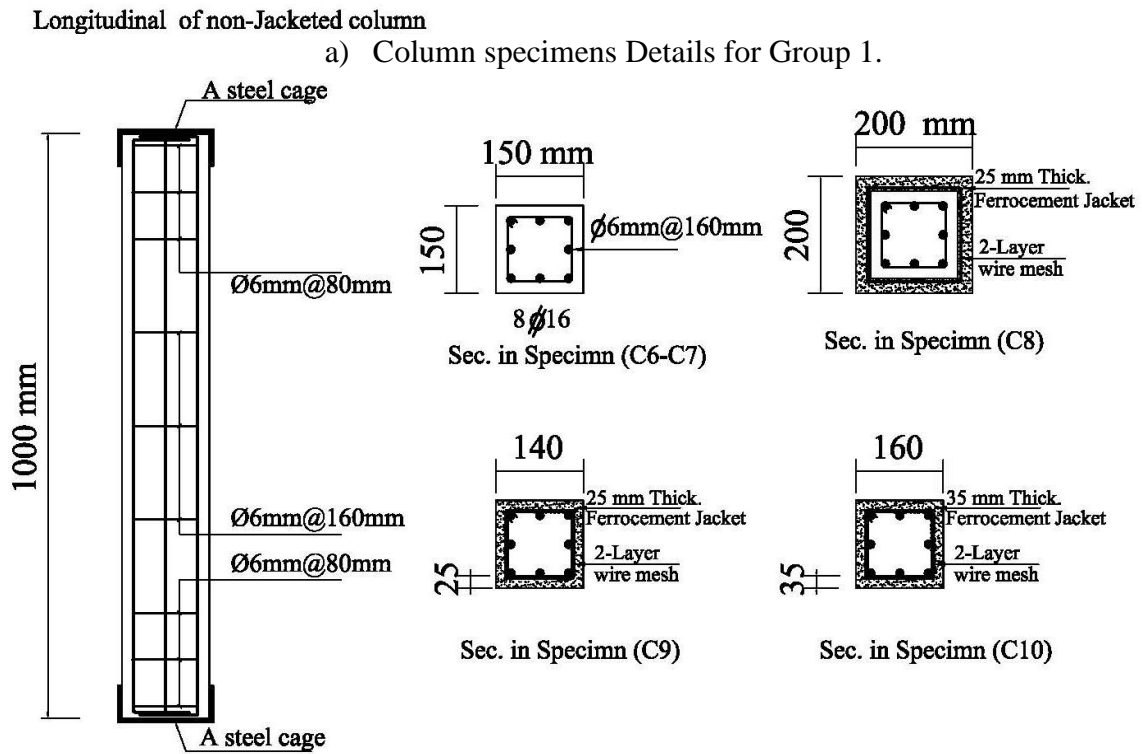
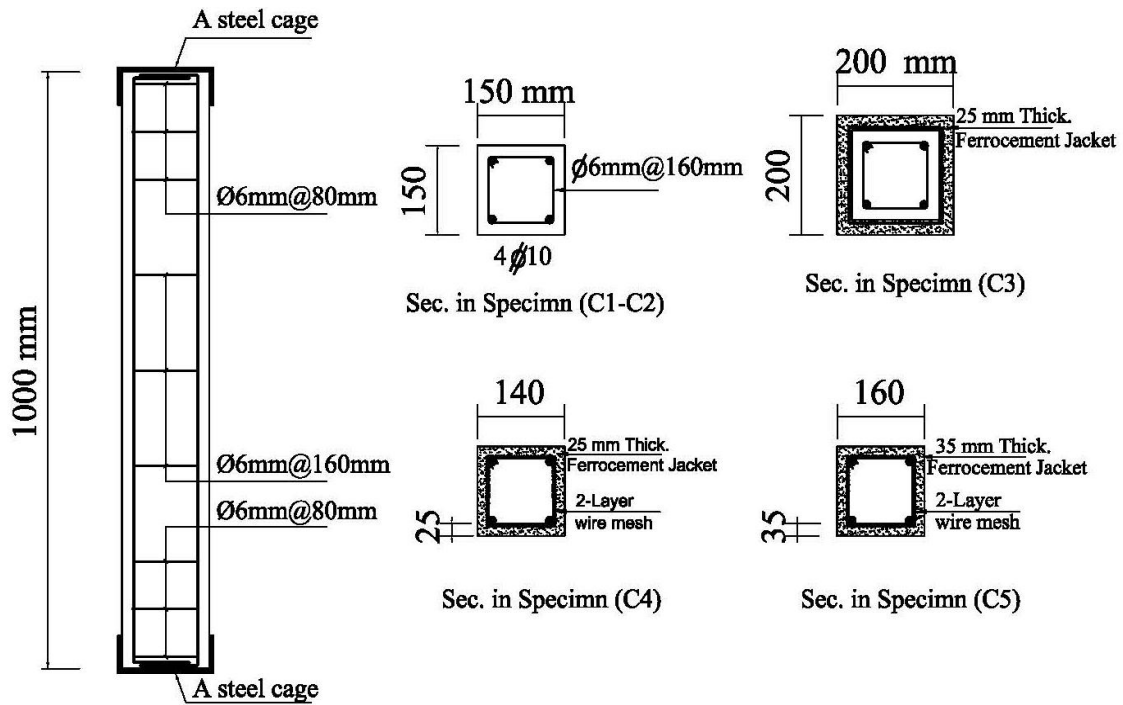


Fig. 1: Columns designations, dimensions and reinforcement arrangement.

For the heated specimens, all columns were heated to a uniform temperature of 300 °C for 3 hours before allowing to cool down. Table 2 gives the descriptions and parametric studies for all tested columns.

Table 2: Specimen nomination.

Group	specimen	Column condition	longitudinal reinforcement ratio ($\mu\%$)	Ferrocement thickness (mm)	No of wire mesh
Group 1	C1	Unheated/non-jacketed		----	----
	C2	Post-heated/non-jacketed		----	----
	C3	Ferrocementconfinement/ Pre-heated	1.3	25	2
	C4	Post-heated/Ferrocement repaired		25	2
	C5	Post-heated/Ferrocement repaired		35	2
Group 2	C6	Unheated/non-jacketed		----	----
	C7	Post-heated/non-jacketed		----	----
	C8	Ferrocementconfinement/ Pre-heated	7	25	2
	C9	Post-heated/Ferrocement repaired		25	2
	C10	Post-heated/Ferrocement repaired		35	2

4.1 Test procedures,Instrumentation and Test Setup

After casting and curing the column specimens,the testing procedure has been executed according to the following steps as shown in Fig. 2.

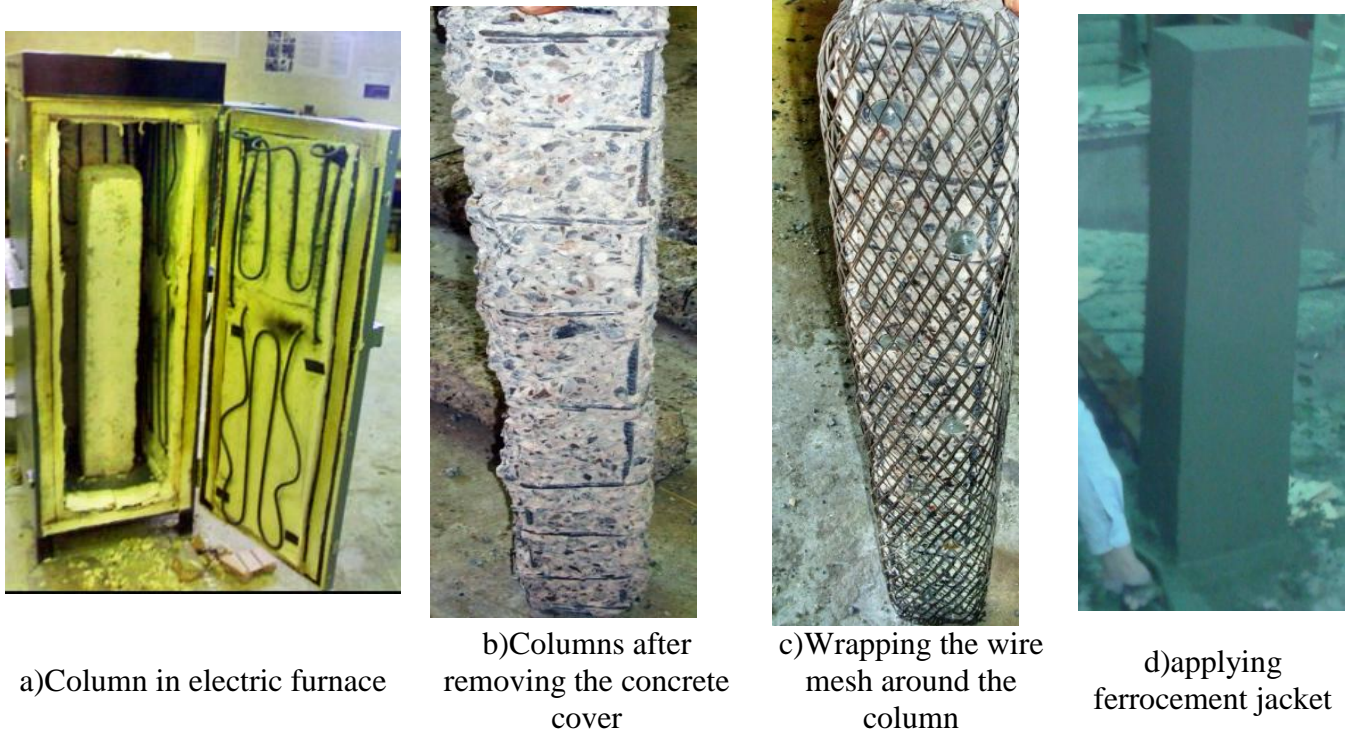


Fig. 2: Stages of preparing ferrocement jacket.

- Stage one;the column specimens (C2, C4, C5, C7, C9, and C10) were heated in an electric furnace to a temperature of 300°C for 3 hours.

- Stage two; repairing of damaged heat columns with ferrocement. Prior to applying the ferrocement, the cover of the heated columns was removed and cleaned to get rid of the dust. The required wire meshes were cut and wrapped around the entire column. Then the primer bonding mortar was plastered on column sides to give high adhesion between the concrete core of the column and the next layer (Matrix). Finally applying the mortar layer.
- Stage three; the confined columns (C3 and C8) were heated in an electric furnace to a temperature of 300°C for 3 hours.
- Step four; all specimens were tested under concentric loading mode. Before testing all columns were fixed by using a steel cage connected to the upper and lower ends of each column in order to avoid stress concentration problems and to ensure distribution the load uniformly. The compressive load was applied using a 1000 kN capacity hydraulic jack in a monotonically increasing manner. The details of the test setup are shown in Fig. 3.



Fig. 3: Loading frame and test set up.

4. Numerical analysis using finite element implementation

All tested columns were simulated using the finite element package ANSYS 13 [27] in order to compare the experimental results with the numerical ones. The results of the experimental work were used to confirm the finite element models.

4.1 Defining material properties

The current simulation model takes into consideration both the geometry and non-linearity of the material. In this study, the solid65 element was used to simulate the concrete and the mortar. The solid65 element is defined by eight nodes, where each node has three degrees of freedom (translations in the X, Y, and Z directions). This element has cracking and crushing capabilities. Fig. 4 presents node's locations and the coordinate system of SOLID65. On the one hand, the Link-8, a 3D link element, is used to model the transverse and the longitudinal reinforcement. While the 3D Solid-45 element is used to represent the reinforced concrete solid element as well as modelling the steel wire mesh. Table 3 shows the properties for each element.

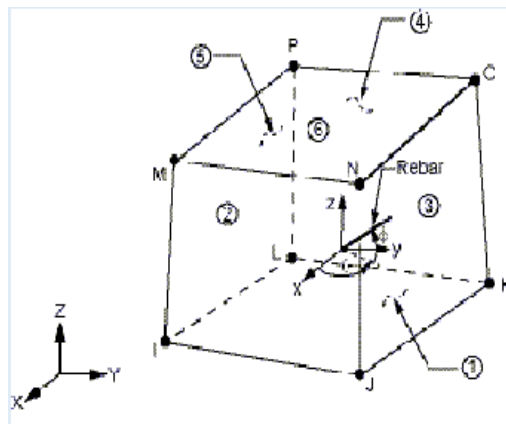


Fig. 4: Node locations and the coordinate system of solid65.

Table 3: Material properties for each element.

Material	Element type	Material properties	
Concrete	Solid 65	Elastic modulus (E_x)	$4400 \sqrt{f_{cu}} \text{MPa}$
		Uniaxial crushing stress (f_c')	$f_{cu} \text{MPa}$
		Uniaxial tensile stress (f_t)	$0.6 \sqrt{f_{cu}} \text{MPa}$
		Poisson's ratio (ν)	0.20
		Shear coefficient for open shear (β_t)	0.20
		Shear coefficient for closed shear (β_c)	0.85
Longitudinal reinforcement	Link 8	Elastic modulus (E_x)	195000 MPa
		Yield stress (f_y)	412 MPa
		Tensile Strength	628 MPa
		Poisson's ratio (ν)	0.30
Stirrups	Link 8	Elastic modulus (E_x)	200000 MPa
		Yield stress (f_y)	282 MPa
		Tensile Strength	459 MPa
		Poisson's ratio (ν)	0.30
Mortar	Solid 65	Elastic modulus (E_x)	24100 MPa
		Uniaxial crushing stress (f_{cu})	35 MPa
		Uniaxial tensile stress (f_t)	3.60 MPa
		Poisson's ratio (ν)	0.20
		Shear coefficient for open shear (β_t)	0.02
		Shear coefficient for closed shear (β_c)	0.4
Wire Mesh	Solid 45	longitudinal Elastic modulus	175000 MPa
		Yield stress (f_y)	370 MPa
		Poisson's ratio (ν)	0.30
		Thickness	1.35 mm

Numerical Modelling of Columns

Fig. 5 shows ANSYS numerical model representation of the experimental specimens. In order to gain accurate results, the full height of the columns is considered for the creation of the models with a mesh size equivalent to 50 mm.

4.2 Boundary conditions and Loading Scheme

The experiment conditions have been used to define the boundary conditions while the load application of the finite element analysis has been described to simulate the actual loading sequence. The columns were modelled in the vertical direction, where the horizontal translations of all base joints were restrained in the three directions. In a nonlinear environment, a displacement control incrementally increasing loading was monotonically applied on the top face of the column.

5. The Prediction Equation

In order to predict the ultimate failure load of unwrapped and wrapped heated columns by ferrocement, the following prediction equation was suggested.

$$P_{uf} = 0.65 f_{cu} (A_c - A_{st}) + f_y A_{st} + 0.65 f_{cuf} A_{cf} + A_{sf} f_{yf}$$

P_{uf} : Ultimate Failure Load

f_{cu} : Compressive strength of concrete after heating

A_c : Gross area of the core of concrete

f_{cuf} : Compressive strength of cement mortar

f_y : Yield strength of steel

A_{cf} : Area of cement mortar

A_{st} : Area of longitudinal steel

f_{yf} : Yield strength of wire mesh

A_{sf} : Area of steel wire mesh

This equation was expected to give an estimate failure loads for other values of the volume fraction of reinforcement, values of ferrocement thickness, and mortar grade.

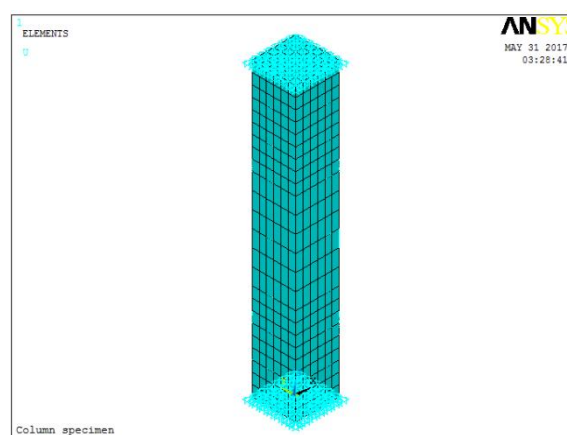


Fig. 5: ANSYS numerical model.

6. Results and Discussion

6.1 Experiment Results

The main results of this experimental program to be discussed are the ultimate load carrying capacity, the crack propagation and mode of failure of the tested specimens.

6.1.1 Ultimate Failure Load

All columns were tested until they reached their failure load. The failure loads of the first and second group are plotted in Fig. 6 and Fig. 7, respectively. Furthermore; Table 4 summarizes all the test results. It can be shown that after heating, the failure load of columns was reduced significantly. However, a considerable load was restored after wrapping heated columns by ferrocement. The ultimate load carrying capacities of under and over reinforced columns were reduced by up to 45% and 33% respectively after heating. It can be seen that the axial ultimate load of heated confined columns was reduced by 13% and 8% for both under and over reinforced columns respectively. The results indicated that repairing post-heated columns, caused 63% and 41% increase in ultimate load for under and over reinforced columns respectively. In the case of confined pre-heated columns, it can be seen that ferrocement strengthening technique was influential in protecting the columns. The decrease in failure load of the post-heated over reinforced columns is less than under reinforced columns.

Table 4: Summary of the test results of specimens.

Group	No. of specimen	Compressive strength of heated column	% Losses in compressive strength	Failure Load (kN)	% Increase in the column failure load above heated column	% Reduction in the column Failure Load compared with unheated column
Group 1	C1	27	0.0	543	82.2	0.0
	C2	12	56	298	0.0	45.1
	C3	25	7.5	472	58.4	13.1
	C4	12	56	429	44.0	21.0
	C5	12	56	485	62.8	10.7
Group 2	C6	27	0.0	917	49.8	0.0
	C7	12	56	612	0.0	33.3
	C8	25	7.5	846	38.2	7.7
	C9	12	56	795	29.9	13.3
	C10	12	56	861	40.7	6.1

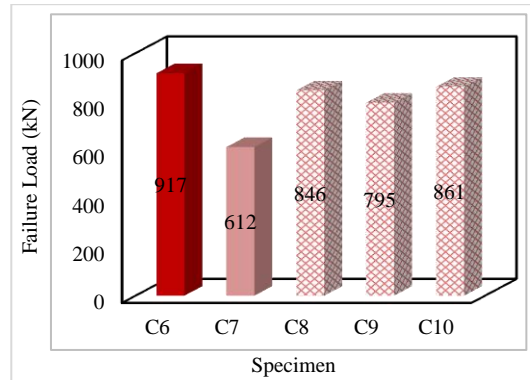
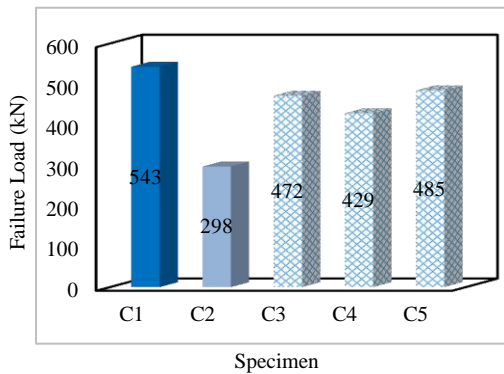


Fig. 6: Failure load of columns for group 1.

Fig. 7: Failure load of columns for group 2.

6.1.2 Failure Modes and Cracking Patterns

The surface of the columns was carefully observed following heating. Random small cracks on the surface of each column were observed. Fig. 8 shows the damages observed at failure load. Generally, a typical crushing mode of failure was observed for all the tested specimens. The most tested columns were failed at their end or ends due to the effects of accumulation and concentration of stresses in such regions. As the load increases, inclined cracks started to appear near the bottom of the column head, increasing in number and getting wider in aperture until failure occurs suddenly. Also, it can be seen that the failure occurs due to the collapse of concrete strength at the lower part of columns. For post-heated repaired columns, the failure was initiated by vertical hairline cracks in the mortar of ferrocement due to the failure of wire mesh throughout the height of the column specimens. A segment of ferrocement mortar of pre-heated confinement columns was separated after heating in an electric furnace.



Failure mode for C1



Cracks Appeared in post-heated column C2



Failure mode for C4



Failure mode for C5

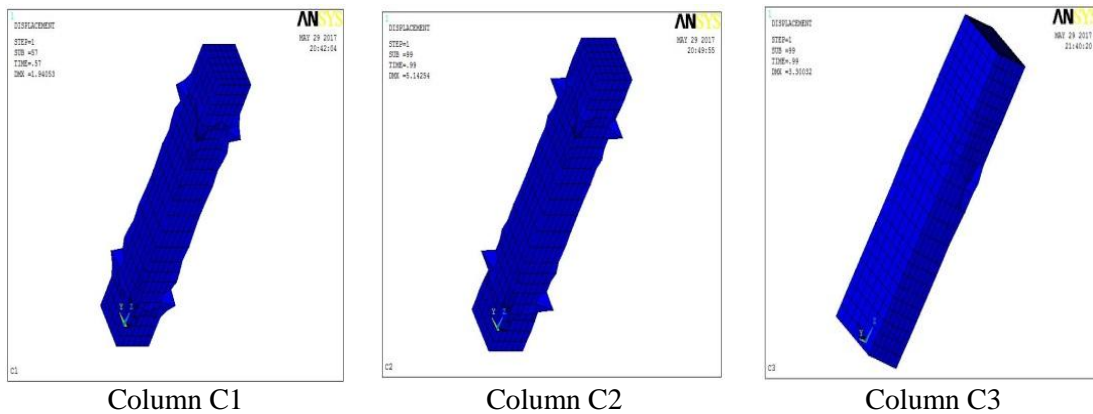


Fig. 8: Failure mode for tested specimens.

7. Numerical Results

7.1 Failure Modes

The deformed shapes for the tested specimens and the concrete cracks at failure load are plotted in Fig. 9. It observed that the unwrapped columns have large deformations in concrete while cracked/crushed concrete elements were located in the near area of the column head with less concentration near the middle of the column's height. It can also be noticed that post-heated columns failed in the middle zones. In all models; cracks started to develop in elements just located under the loading plates and they increased in quantity and width with the increasing load.



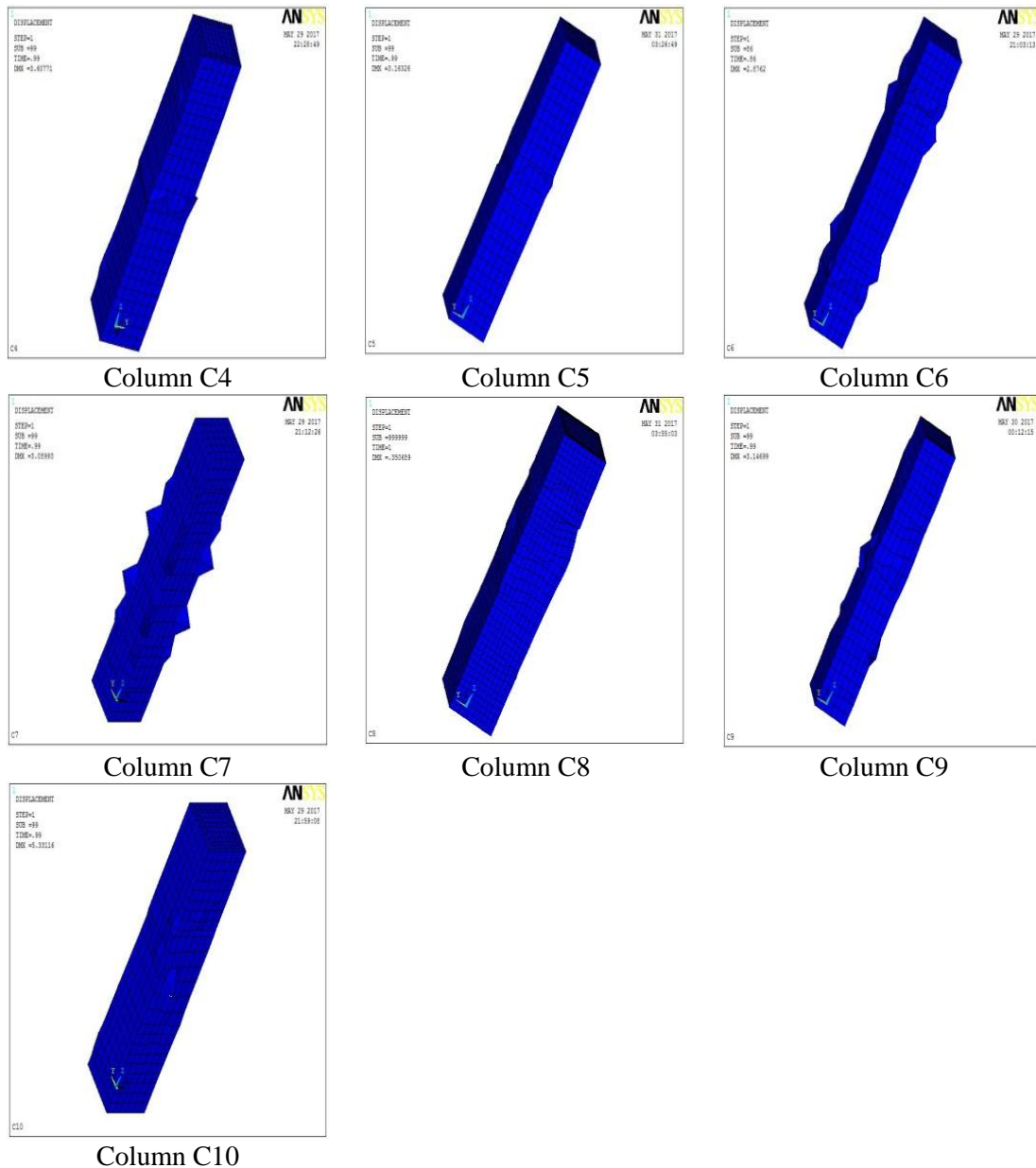


Fig. 9: Deformation of all models at failure load.

8. Comparison Between Experimental, Numerical and Prediction Equation Results

Fig. 10 shows a comparison between experimental, numerical, and prediction design equation results for group 1 and group 2. The ultimate failure loads of experimental, numerical, and prediction design equation results with the ratios between them are tabulated in Table 5. The obtained numerical and prediction formula ultimate loads agree quite well with the experimental ones, although the results slightly overestimate the failure load. In general, the experimental results show higher failure loads for most of the specimens compared to their corresponding finite element models. The maximum errors between experimental and the numerical results are $\pm 5\%$ and the mean value of the ratio between them was 1.013 with a standard deviation 0.025. It can be noticed that the predicted formula gave higher failure load values in comparison to the experimental values except for specimens C1 and C4. The average value of the ratio between experimental and design equation was 97% with standard

deviation 0.046. It can be concluded that the results of finite element analyses are as accurate as those of the proposed formula, with respect to the ultimate load capacity. Finally, from the observation, the finite element program ANSYS is a useful and useable tool to determine the ultimate load capacity of unwrapped or wrapped heated or un-heated columns.

Table 5: Comparison between experimental, numerical and prediction equation results.

Column Specimen	Failure Load (kN)			$\frac{EXP.}{ANSYS}$	$\frac{EXP.}{Equ.}$
	Exp.	ANSYS	Equ.		
C1	543	538	521	1.01	1.04
C2	298	283	286	1.05	1.04
C3	472	488	485	0.97	0.97
C4	429	421	412	1.02	1.04
C5	485	502	489	0.97	0.99
C6	917	886	987	1.03	0.93
C7	612	598	641	1.02	0.95
C8	846	838	923	1.01	0.92
C9	795	789	833	1.01	0.95
C10	861	830	891	1.04	0.97
Average				1.013	1.077
Standard deviation				0.025	0.046

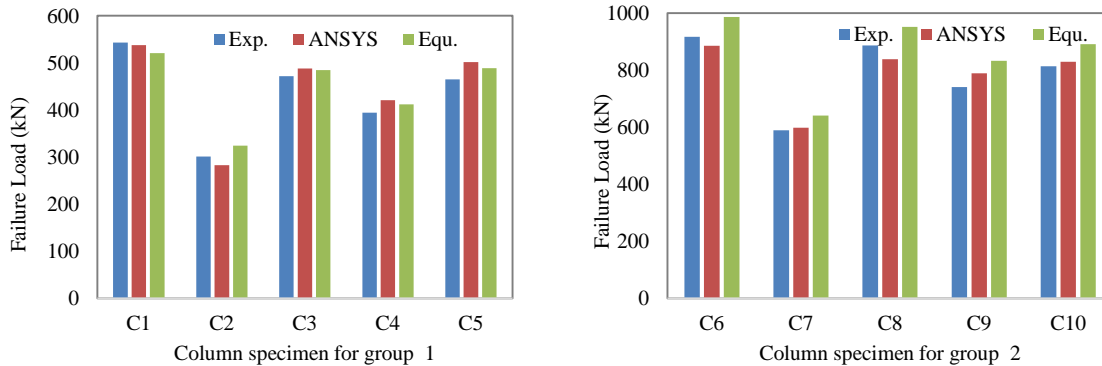


Fig. 10: Comparison between experimental, numerical and Prediction Equation results.

9. Parametric study

9.1 Numerical Models Description

The finite element model was used to extend the parametric study to cover other parameters which have not been investigated experimentally. A total of 60 extra models were analyzed to investigate the efficiency of using ferrocement laminates in repairing post-heated RC columns. The studied parameters were, the ferrocement thickness, mortar grade, the number of steel wire mesh, and the main reinforcement ratio. Five different thicknesses of ferrocement were taken into account (10 mm, 15 mm, 20 mm, 25 mm, and 30 mm). The considered mortar strength were 60 MPa and 90 MPa. The number of weld mesh layers were considered with three different values: (1, 2, and 3 layers). The longitudinal reinforcement was considered with

three different values: (4Φ10,8Φ16). The description of the additional column models are given in Table6.

9.2 Parametric Study Results

Table6 shows the failure loads of the finite element models. On the basis of the numerical results, ferrocement jackets can be used to improve the load carrying capacity of the heated RC columns. The results clearly showed that ferrocement confinement leads to a significant enhancements in the failure loads of the confined columns. The strength of the post-heated wrapped columns is significantly affected by both the ferrocement thickness and mortar strength. It can be seen that increasing the percentage volume of the wire mesh layer subsequently increasing the ultimate load of the columns. It can be noticed that the strength of the heated column with three weld mesh layers greater compared to with that of two layers for the same thickness of slab.

Table 6: The description of the additional column models and results.

Model	Main RFT.	Ferrocement thickness (mm)	No of wire mesh	volume fraction of reinforcement (V_f %)	Compressive strength of mortar (MPa)	Failure Load (kN)	% Increase in the column failure load above heated column
Co	4Φ10	Post-heated/non-jacketed (C2)				283	0.0
C1	4Φ10	10	1	1.86	65	337	19.1
C2	4Φ10	15	1	1.24	65	450.2	59.1
C3	4Φ10	20	1	0.93	65	568.5	100.9
C4	4Φ10	25	1	0.74	65	696.9	146.3
C5	4Φ10	30	1	0.62	65	819.1	189.4
C6	4Φ10	10	2	3.72	65	365.4	29.1
C7	4Φ10	15	2	2.48	65	463	63.6
C8	4Φ10	20	2	1.86	65	586.1	107.1
C9	4Φ10	25	2	1.48	65	735.1	159.8
C10	4Φ10	30	2	1.24	65	862.8	204.9
C11	4Φ10	10	3	5.58	65	374.8	32.4
C12	4Φ10	15	3	3.72	65	506.8	79.1
C13	4Φ10	20	3	2.79	65	591.4	109.0
C14	4Φ10	25	3	2.23	65	742.6	162.4
C15	4Φ10	30	3	1.86	65	903	219.1
C16	4Φ10	10	1	1.86	90	429	51.6
C17	4Φ10	15	1	1.24	90	578.7	104.5
C18	4Φ10	20	1	0.93	90	743.4	162.7
C19	4Φ10	25	1	0.74	90	923.1	226.2
C20	4Φ10	30	1	0.62	90	1087.9	284.4
C21	4Φ10	10	2	3.72	90	457.2	61.6
C22	4Φ10	15	2	2.48	90	610.4	115.7

C23	4Φ10	20	2	1.86	90	780.6	175.8
C24	4Φ10	25	2	1.48	90	937.9	231.4
C25	4Φ10	30	2	1.24	90	1132.5	300.2
C26	4Φ10	10	3	5.58	90	496.7	75.5
C27	4Φ10	15	3	3.72	90	655.5	131.6
C28	4Φ10	20	3	2.79	90	810.5	186.4
C29	4Φ10	25	3	2.23	90	973.4	244.0
C30	4Φ10	30	3	1.86	90	1154.6	308.0
Co	8Φ16	Post-heated/non-jacketed (C7)				598	0.0
C31	8Φ16	10	1	26.8	65	758.2	28.7
C32	8Φ16	15	1	38.9	65	830.8	41.1
C33	8Φ16	20	1	57.9	65	944	60.3
C34	8Φ16	25	1	76.9	65	1058.1	79.6
C35	8Φ16	30	1	97.6	65	1181.6	100.6
C36	8Φ16	10	2	27.2	65	760.4	29.1
C37	8Φ16	15	2	41.9	65	848.8	44.1
C38	8Φ16	20	2	59.5	65	953.7	61.9
C39	8Φ16	25	2	80.8	65	1081	83.5
C40	8Φ16	30	2	104.6	65	1223.7	107.8
C41	8Φ16	10	3	39.6	65	834.7	41.7
C43	8Φ16	15	3	57.9	65	944.1	60.3
C43	8Φ16	20	3	75.5	65	1049.4	78.2
C44	8Φ16	25	3	95.5	65	1169.2	98.5
C45	8Φ16	30	3	114.0	65	1279.5	117.2
C46	8Φ16	10	1	42.1	90	850	44.3
C47	8Φ16	15	1	65.1	90	987.3	67.6
C48	8Φ16	20	1	89.5	90	1133.4	92.4
C49	8Φ16	25	1	119.0	90	1309.5	122.3
C50	8Φ16	30	1	147.7	90	1481.5	151.5
C51	8Φ16	10	2	47.6	90	882.5	49.8
C52	8Φ16	15	2	70.9	90	1022.2	73.5
C53	8Φ16	20	2	95.6	90	1169.5	98.6
C54	8Φ16	25	2	121.1	90	1321.9	124.4
C55	8Φ16	30	2	151.1	90	1501.3	154.9
C56	8Φ16	10	3	56.5	90	935.8	58.9
C57	8Φ16	15	3	80.1	90	1077	82.9
C58	8Φ16	20	3	106.3	90	1233.8	109.5
C59	8Φ16	25	3	131.5	90	1384.5	135.1
C60	8Φ16	30	3	161.5	90	1563.8	165.5

10. Conclusion

Based on the results of this paper obtained using both experimental and theoretical analyses for columns subjected to fire, our conclusions can be drawn as follows:

1. Based on the experimental results, ferrocement confinement is an effective technique to improve the strength of post-heated columns.
2. The ultimate load of post-heated columns reduced down to 45% after exposed to 300 °C for 3 hours. Also, the concrete becomes more porous with appeared a small cracks.
3. The strength of the post-heated columns repaired with ferrocement overlays was increased by 63% and 41% more than the strength of post-heated column with reference to reinforcement ratio.
4. Increasing the ferrocement thickness leads to ultimate load enhancement of repaired columns.
5. The ultimate load of post-heated column wrapped by ferrocement is significantly affected by increasing the thickness of the mortar
6. The reduced in the axial ultimate load of the post-heated column with under-reinforced is more than that of over reinforced column.
7. The failure load of pre-heated columns decreased by 13% after heating, which proved that ferrocement coating is an effective heat insulator.
8. The ultimate loads of both the post-heated and pre-heated columns repaired with ferrocement overlays are characterised with lower values compared to the original strength of un-heated columns.
9. The reduction in axial load of the post-heated over reinforced columns is less than that of under-reinforced columns.
10. Generally, the theoretical results obtained using both the finite element analysis and prediction formula are in good agreement with the experimental values. The ANSYS program and predicted formula can be utilized to determine the effect of variables not studied experimentally.

Acknowledgements

The authors would like to express their thanks to the staff of the concrete research and material properties laboratory of the Faculty of Engineering, Fayoum University. In addition, the authors are grateful to Dr. Ahmed H. Mansi for his useful conversations and important suggestions which helped improving the quality of this manuscript.

References

- [1] The American Concrete Institute, "Guide for design, construction & repair of ferrocement," The American Concrete Institute, Michigan, USA, 1993.
- [2] Abdullah and K. Takiguchi, "An investigation into the behavior and strength of reinforced concrete columns strengthened with ferrocement jackets," *Cement and Concrete Composites*, vol. 25, no. 2, pp. 233 - 242, 2003.
- [3] A. Kaish, M. Jamil, S. Raman and M. Zain, "Axial behavior of ferrocement confined cylindrical concrete specimens with different sizes," *Construction and Building Materials*, vol. 78, pp. 50-59, 2015.
- [4] A. Kaish, M. Alam, M. Jamil, M. Zain and M. Wahed, "Improved ferrocement jacketing for restrengthening of square RC short column," *Construction and Building Materials*, vol. 36, pp. 228-237, 2012.
- [5] S. Mourad and M. Shannag, "Repair and strengthening of reinforced concrete square columns using ferrocement jackets," *Cement and concrete composites*, vol. 34, no. 2, pp. 288-294, 2012.

- [6] A. Al-Sibahy, "Behaviour of Reinforced Concrete Columns Strengthened with Ferrocement under Compression Conditions: Experimental Approach," *World Journal of Engineering and Technology*, vol. 4, no. 4, pp. 608-622, 2016.
- [7] M. Salih and C. Arunkumar, "Strengthening of reinforced concrete column using Jacketing Technique," in *International Conference on Engineering Innovations and Solutions*, 35-38, 2016.
- [8] J. Malhotra, "Behaviour of RCC columns confined with ferrocement," Thapar University, 2013.
- [9] S. Sirimontree, B. Witchayangkoon and K. Lertpocasombut, "Strengthening of Reinforced Concrete Column via Ferrocement Jacketing," *American Transactions on Engineering and Applied Sciences*, vol. 4, no. 1, pp. 39-47, 2015.
- [10] V. Shinde and J. Bhusari, "Response Of Ferrocement Confinement On Behavior Of Concrete Short Column," *IOSR Journal of Mechanical and Civil Engineering (IOSR-JMCE)*, p. 24–27, Shinde.
- [11] M. Soman and M. Veena, "Repair and rehabilitation of RC short square columns using improved ferrocement jacketing," in *International Journal of Earth Sciences and Engineering*, 2015.
- [12] L. Abdel-Hafez, A. Abouelezz and A. Hassan, "Behavior of RC columns retrofitted with CFRP exposed to fire under axial load," *HBRC Journal*, vol. 11, no. 1, pp. 68-81, 2015.
- [13] J. Rodrigues, L. Laím and A. Correia, "Behaviour of fiber reinforced concrete columns in fire," *Composite Structures*, vol. 92, no. 5, pp. 1263-1268, 2010.
- [14] K. K. Venkatesh, A. B. Luke and F. G. Mark, "Experimental evaluation of the fire behaviour of insulated fibre-reinforced-polymer-strengthened reinforced concrete columns," *Fire Safety Journal*, vol. 41, no. 7, pp. 547 - 557, 2006.
- [15] D. Cree, E. Chowdhury, M. Green, L. Bisby and N. Bénichou, "Performance in fire of FRP-strengthened and insulated reinforced concrete columns," *Fire Safety Journal*, vol. 54, pp. 86 - 95, 2012.
- [16] L. Bisby, J. Chen, S. Li, T. Stratford, N. Cueva and K. Crossling, "Strengthening fire-damaged concrete by confinement with fibre-reinforced polymer wraps," *Engineering Structures*, vol. 33, no. 12, pp. 3381 - 3391, 2011.
- [17] M. Yaqub and C. Bailey, "Repair of fire damaged circular reinforced concrete columns with FRP composites," *Construction and Building Materials*, vol. 25, no. 1, pp. 359 - 370, 2011.
- [18] E. Chowdhury, "Behaviour of fibre reinforced polymer confined reinforced concrete columns under fire condition," Queen's University, Ontario, Canada, 2009.
- [19] A. Parvin and D. Brighton, "FRP composites strengthening of concrete columns under various loading conditions," *Polymers*, vol. 6, no. 4, pp. 1040-1056, 2014.
- [20] Y. Al-Kamaki, R. Al-Mahaidi and I. Bennetts, "Experimental and numerical study of the behaviour of heat-damaged RC circular columns confined with CFRP fabric," *Composite Structures*, vol. 133, p. 679–690, 2015.
- [21] H. Z. El-Karmoty, "Thermal protection of reinforced concrete columns strengthened by GFRP laminates (experimental and theoretical study)," *HBRC Journal*, vol. 8, no. 2, pp. 115 - 122, 2012.
- [22] Z. C. Tetta and A. B. Dionysios, "TRM vs FRP jacketing in shear strengthening of concrete members subjected to high temperatures," *Composites Part B: Engineering*, vol. 106, pp. 190 - 205, 2016.

- [23] M. Yaqub, C. Bailey and P. Nedwell, "Axial capacity of post-heated square columns wrapped with FRP composites," *Cement and Concrete Composites*, vol. 33, no. 6, pp. 694 - 701, 2011.
- [24] M. Yaqub and C. Bailey, "Seismic performance of shear critical post-heated reinforced concrete square columns wrapped with FRP composites," *Construction and Building Materials*, vol. 34, pp. 457 - 469, 2012.
- [25] C. Bailey and M. Yaqub, "Seismic strengthening of shear critical post-heated circular concrete columns wrapped with FRP composite jackets," *Composite Structures*, vol. 94, no. 3, pp. 851-864, 2012.
- [26] M. Yaqub, C. Bailey, P. Nedwell, Q. Khan and I. Javed, "Strength and stiffness of post-heated columns repaired with ferrocement and fibre reinforced polymer jackets," *Composites Part B: Engineering*, vol. 44, no. 1, pp. 200 - 211, 2013.
- [27] ANSYS, "ANSYS User's Manual and Help Revision 13," ANSYS Inc., PA, USA, 2010.